Warming and Freshening of the Pacific Inflow to the Arctic from 1990-2019 implying dramatic shoaling in Pacific Winter Water ventilation of the Arctic water column

R. A. Woodgate[1] and C. Peralta-Ferriz[1]

[1]University of Washington, Seattle, USA.

Corresponding author: Rebecca Woodgate (woodgate@uw.edu)

Key Points:

- In situ hourly 1990-2019 data show Bering Strait flow increases ~0.01Sv/yr, cutting Chukchi residence time by ~1.5 months to ~5 months now
- Spring/fall warming, ~0.1C/yr, yields monthly means 2-4C above climatology and warm waters persist for >7 months (previously 5.5 months)
- Pacific Winter Water (PWW) freshening (to < summer salinities) shoals Arctic ventilation, so that PWW no longer renews the cold halocline

Key Words:

Bering Strait	Interannual Change	Pacific-Arctic Connections
Sea ice	Ocean warming	Arctic Halocline

Index Terms:

9315 Arctic region (0718, 4207)
4215 Climate and interannual variability (1616, 1635, 3305, 3309, 4513)
1621 Cryospheric change (0776)
4513 Decadal ocean variability (1616, 1635, 3305, 4215)
4262 Ocean observing systems

Orcid:

Rebecca Woodgate https://orcid.org/0000-0002-8901-6783
Cecilia Peralta-Ferriz https://orcid.org/0000-0002-9537-0973

Submitted to Geophysical Research Letters January 2021, Revised March 2021; Accepted April 2021

Abstract

The Pacific inflow to the Arctic traditionally brings heat in summer, melting sea ice; dense waters in winter, refreshing the Arctic's cold halocline; and nutrients year-round, supporting Arctic ecosystems. Bering Strait moorings from 1990-2019 find increasing (0.010±0.006Sv/yr) northward flow, reducing Chukchi residence times by ~1.5 months over this period (record maximum/minimum ~7.5 and ~4.5 months). Annual mean temperatures warm significantly (0.05±0.02°C/yr), with faster change (~0.1°C/yr) in warming (June/July) and cooling (October/November) months, which are now 2-4°C above climatology. Warm (≥0°C) water duration increased from 5.5 months (1990s) to over 7 months (2017), mostly due to earlier warming (1.3±0.7days/yr). Dramatic winter-only (January-March) freshening (0.03psu/yr), makes winter waters fresher than summer waters. The resultant winter density change, too large to be compensated by Chukchi sea-ice processes, shoals the Pacific Winter Water (PWW) equilibrium depth in the Arctic from 100-150m to 50-100m, implying PWW no longer ventilates the Arctic's cold halocline at 33.1psu.

Plain Language Summary

The Bering Strait is the only oceanic link between the Pacific and Arctic Oceans. The typically northward flow through the strait carries Pacific oceanic nutrients to the Arctic, vital for ecosystems. The flow varies seasonally in temperature and salinity. In spring/summer, it brings warm waters that start the melt-back of Arctic sea ice. In winter, it carries cold waters that traditionally sink deeper (100-150m) into the Arctic, well below the summer waters. Annually-serviced instrumentation moored to the sea floor measured (hourly) the flow and properties in the strait from autumn 1990 to summer 2019. We find the flow is increasing significantly, reducing by ~1.5 months the time taken to reach the Arctic from the strait (now ~5 months). Summer waters are now 2-4°C warmer than typical in the 1990s and warm for longer (7 months compared to 5.5 months). In winter, waters are dramatically fresher than before, now fresher than in summer. This change means the winter waters can no longer sink so deep in the Arctic - now only 50-100m, the same depth as the summer waters. This not only means oceanic nutrients are available closer to the surface, but may also restructure how the upper Arctic Ocean mixes.

1 Introduction

The Pacific inflow to the Arctic Ocean, approximately 1Sv (1Sv = 10^6 m^3/s) of water entering through the narrow (~85km wide), shallow (~50m deep) Bering Strait, has multiple impacts on the Arctic and beyond [*Woodgate*, 2018]. In winter, colder Pacific waters traditionally renew the Arctic's cold halocline layer, inhibiting upward heat transfer from the Arctic's deeper, warmer Atlantic waters [*Aagaard et al.*, 1981]. However, in spring to autumn, the Pacific inflow, being warmer (and traditionally fresher) [*Woodgate et al.*, 2005b], carries heat which triggers the onset of western Arctic ice-melt and, by entering the Arctic shallower than the cold halocline, provides a year-round subsurface heat source to the surface of roughly half the Arctic Ocean [*Woodgate et al.*, 2010].

Since Pacific waters are the major source of Arctic nutrients [*Walsh et al.*, 1997], their volume and reach (horizontally and vertically) have implications for all Arctic ecosystems.

Moreover increased flow hastens northwards advection of species [e.g., *Levine et al.*, 2020] and reduces Chukchi Sea residence times.

In these times of dramatic Arctic change [*Thoman et al.*, 2020], prior (1990-2015) Bering Strait data [*Woodgate*, 2018] show increasing northward flow (~0.009Sv/yr), warming (~0.03°C/yr), and winter freshening (~0.02psu/yr). Extending this time-series to summer 2019, we now find not just continued high flow (Section 3), but also substantially increasing warmth (Section 4), and remarkably enhanced winter and year-round freshening, implying dramatic shoaling of the Pacific winter ventilation of the Arctic (Section 5).

2 Data and Methods

2.1 Bering Strait Mooring Data

From autumn 1990 to summer 2019, year-round subsurface moorings have recorded (typically hourly) near-bottom (~35-45m depth) temperature, salinity, and velocity at sites either in the Bering Strait (some of A1, A2 and A4) or ~35km north of the strait (A3) (Figure 1a, overview in *Woodgate et al.*, [2015]). Deployments are contiguous (except for summer 1996-1997), although data dropouts in the 1990s prevent some annual mean calculations (Figure 1). Data indicate strong seasonal cycles in all properties [*Woodgate et al.*, 2005b] (climatology in Figure 2), seasonal stratification and coastal currents [*Woodgate and Aagaard*, 2005; *Woodgate et al.*, 2010]. *Woodgate et al*., [2018] show the total strait transport and properties can be reasonably estimated from data at site A3 (the "climate" site), making corrections (~4% in volume transport and 10-20% in heat/freshwater transports) for stratification and the Alaskan Coastal Current (ACC), a warm, fresh current present seasonally (July-December) along the Alaskan coast [*Paquette and Bourke*, 1974]. Both the ACC and stratification have been directly measured since 2000 and 2007 respectively, although with some gaps. For our current study of long-term trends, we use only the much longer near-bottom time-series, noting that the shorter ACC and stratification time-series show either no significant change or change that confirms/enhances the trends in the near-bottom data.

2.2 Wind, Sea Surface Temperature, and Sea-ice Data

We use 6-hourly National Centers for Environmental Prediction (NCEP) reanalysis surface winds ([*Kalnay et al.*, 1996], https://psl.noaa.gov) (4-pt average around A3, Figure 1a); daily NOAA/OAR/ESRL PSL High (0.25°) Resolution blended Sea Surface Temperature (SST) ([*Reynolds et al.*, 2007], https://psl.noaa.gov), averaged over a ~40km square region centered on A3; and daily SSM/I National Snow and Ice Data Center ice concentrations ([*Cavalieri et al.*, 1996], https://nsidc.org/data) interpolated to A3.

2.3 Quantification of volume, heat and freshwater fluxes, and forcing terms

Quantification of fluxes, forcing terms and uncertainties are described in *Woodgate* [2018]. In summary:

Total northward volume flux is calculated from A3 near-bottom northward velocity, assuming homogenous flow through a cross-section area of 4.25km^2. *In situ* data [*Woodgate et al.*, 2015] confirm velocity homogeneity apart from in the enhanced flow of the seasonal ACC,

which may add ~0.04Sv to the total transport calculation [*Woodgate*, 2018], an addition included in our estimated uncertainties.

There is a long-standing understanding that the throughflow is driven by a sea surface height gradient between the Pacific and the Arctic [*Coachman and Aagaard,* 1966], generally opposed by winds in the strait, which are often strong enough to reverse the flow. A linear best fit of northward flow to the 6-hourly wind at heading 330° in the strait (correlated at r~0.8 with the northward flow) splits the flow into the local wind-driven and far-field driven components [*Woodgate et al.*, 2005a; *Woodgate*, 2018]. The far-field component (frequently called the "pressure-head") is thus the flow variability unexplained by the local wind.

As we seek to quantify the oceanic heat deposited in the Arctic (e.g., to melt ice), we calculate heat fluxes relative to the temperature of Pacific Waters leaving the Arctic viz., approximately at freezing [*Steele et al.*, 2004], here -1.9 °C. To the base heat flux calculation from hourly near-bottom A3 data, we add corrections for stratification (using daily SST data and mixed layer depth estimates of 10 or 20m) and the ACC, taken as an annual mean constant of $1x10^{20}$J/yr [*Woodgate et al.*, 2010]. (The shorter ACC (A4) time-series, 2002 to 2019 with some gaps, show no significant trends in annual mean near-bottom temperature.)

To estimate the freshening effect of Pacific Waters on the Arctic, we calculate freshwater fluxes relative to the mean Arctic Ocean salinity, 34.8psu [*Aagaard and Carmack*, 1989], again from hourly near-bottom A3 data. Again lacking sufficient data coverage of the ACC and stratification for the entire time-series (and noting the lack of trends in existing annual mean data), we use constant corrections (800-1000km^3/yr) to account for stratification and ACC contributions to the freshwater flux.

For all terms we consider annual (calendar year) means (from 1991 to 2018) (Figure 1), and monthly mean changes, and 30-day smoothed data (Figure 2) (from autumn 1990 to summer 2019). Only linear trends significant at ≥95% are considered. Final uncertainties are order 10-20%. Figure 1 annual means are shown with standard errors of anomalies from a record-length seasonal cycle (computed at native time-resolution), estimating degrees of freedom from the data's integral timescale [*Woodgate*, 2018].

3 Increasing volume transport and decreasing residence time in the Chukchi Sea

Figure 1b shows annual mean transports through the strait from 1990 to 2018 estimated from A3 (black) and A2 (grey). While strong interannual variability is evident, there is also a significant increasing trend since the start of the record (A3 data 1991-2018: 0.010±0.006Sv/yr), with a stronger trend since 2000 (0.016±0.008Sv/yr). This indicates that the similar trends to 2015 reported by *Woodgate* [2018] are continued and more significant in the newer data.

A decomposition into the annual transports of warm and cold waters (taking warm as greater than or equal to 0°C) (red and blue lines in Figure 1b respectively), shows that, averaged over a year, almost all the increasing flow is warmer than 0°C, increasing oceanic heat transported to the Arctic (Section 4).

Splitting the transport into local wind-driven and pressure-head terms suggests that, on the decadal scale, the flow increase is still due to change in the far-field (pressure-head) forcing (green circles, Figure 1b) with no significant trend in the local wind contribution (brown

triangles). Note, however, that since 2014, local wind promotes flow increase, while the far-field term drives reducing flow. This supports the (unsurprising) hypothesis that the throughflow has multiple important drivers. Here we consider only the split into local and far-field (pressure-head) drivers. A study of satellite ocean mass data [*Peralta-Ferriz and Woodgate*, 2017] further divides the pressure-head term into components driven by winds over the East Siberian Sea (dominant in summer) and the Bering Sea (dominant/equal in winter), while both a synthesis of observations and simple modeling [*Danielson et al.*, 2014] and an ice-ocean adjoint model [*Nguyen et al.*, 2020] suggest a role also for winds over shelves which are upstream of the Bering Strait in the sense of shelf wave propagation (i.e., the Bering Sea and the Russian Arctic shelf seas) [*Danielson et al.*, 2020a].

A monthly decomposition of trends in northward transport (Figure 2a, column 1) shows significantly increasing trends in several months throughout the year. Thirty-day smoothed data from recent years (red, Figure 2a, columns 2-4) indicate most months are greater than the 1990-2004 climatology (black, [*Woodgate et al.*, 2005b]). Significant trends throughout the year (not shown) are seen in the pressure-head term as per *Woodgate* [2018], while monthly trends in the local wind term (not shown) are insignificant except in May and June.

While the annual mean transport change may appear small in absolute terms (Figure 1), it represents a sizeable (order 50%) change in the flow and corresponds to major change in residence time in the Chukchi. Assuming (conservatively) that the entire Chukchi is fed from the Bering Strait, we estimate a linear trend of ~1.5 month reduction over the observational period, with the extreme values from 0.7Sv (2001) to 1.2Sv (2014) , equivalent to residence time changes of ~7.5 to ~4.5 months [*Woodgate*, 2018]. These are substantial differences for ecosystems being advected through the region. Note also that the Bering Strait is the only Arctic oceanic gateway showing significant trends over the observational period [*Østerhus et al.*, 2019].

4 Warming, increasing heat fluxes and open water, and their influence on solar heating of the Chukchi

Figure 1c shows annual mean near-bottom temperatures at A3 (black) and A2 (grey), and SST near A3 (red). The remarkable warmth of recent years is clearly evident in all data, but most marked in the near-bottom data, which represent the bulk of the water column. The record length (1991-2018) trend (barely significant to 2015 at A3 and not significant in SST [*Woodgate*, 2018]) is now clearly significant in A3 near-bottom data (0.05±0.02°C/yr) and barely significant in SST (0.02±0.02°C/yr). A2 temperature trends are also now significant (0.03±0.02°C/yr). Whereas in the 1990s, annual mean A3 temperatures were frequently below 0°C, all years since 2014 show positive annual mean temperatures.

Seasonally (Figure 2b, first column), significant warming is found in all months. The smallest trends are in winter when the water is at the freezing point and thus these warming trends reflect freshening, which is discussed in Section 5. Although there is significant warming in all the warm season, the largest trends are found in the "shoulder" seasons, the months of seasonal warming (June/July) and cooling (October/November). This reflects the earlier onset of warming and later onset of cooling. These changes are dramatic - in 2017 and 2018, mean June temperatures are 4°C, compared to a climatology of 2°C; in 2016 and 2018, mean

October/November temperatures are 3-4°C warmer than climatology (Figure 2b, columns 2-4). Similarly large changes are seen in the 30-day smoothed SSM/I ice concentration near A3 (Figure 2g) - for 2016, 2017 and 2018, June ice concentrations (climatologically ~50%) are mostly zero; in 2016 and 2017, December ice concentrations (climatologically ~75%), are ~20% and 5% respectively.

Figures 1d/1e (black) show the first/last day when the 30-day smoothed A3 near-bottom temperatures are above 0°C. Despite individual anomalous years (e.g., 2012, anomalously cold, late to warm, early to cool), in general over the 29 years of the data, warming onset has moved from early July to late May (earlier by 1.3±0.7days/yr). Cooling onset trends are both smaller and less significant (later by 0.6±0.6days/yr), with a clear trend to later cooling only visible since around 2012. Before this, mid November marked the average time of cooling to 0°C in the strait in the 30-day smoothed data. However, in four of the last five complete years (2014-2018), warmer waters have remained (in the 30-day mean) until mid December, with hourly data (not shown) documenting waters warmer than 0°C in the strait until early January in winters 2016-2017 and 2018-2019.

Similar changes are seen in the dates of retreat and advance of sea ice (Figure 1d/1e, blue), which are well correlated with water warming (r=0.74) and cooling (r=0.81) times. Sea-ice trends over the 28-year period are significant, although the melting trend (earlier by 0.5±0.4days/yr) is seemingly around half the water warming trend, while the trend to later freezing (later by 0.9±0.5days/yr) is perhaps stronger than the trend to later cooling. This suggests that water warming is not just due to local ice retreat, indicative of the more likely advective driving of warming in the strait, and similarly that the onset of freezing is only partly driven by the change in water temperature.

Combination of earlier warming and later cooling increases the number of days of warm water in the strait (Figure 1f, trend 2.0±1.0days/yr). Previously the warm period was around 5.5 months, but the last 3 years have more than 6 months of warm waters, and 2017 was warm for over 7 months. Similarly, the ice free season in the strait is increasing, by 1.4±0.6days/yr.

These changes have obviously major impacts on local inhabitants, ecosystems and shipping in the region. But there is an additional physical amplification of this warming via shortwave (SW) input to the region being absorbed into the water primarily during ice-free times. Prior work [*Woodgate et al.*, 2010] shows the SW absorbed within the Chukchi Sea is currently comparable to the oceanic heat carried through the strait. But available SW peaks around the 1st June, about the time of current ice retreat (Figure 1d). Thus earlier ice melt will substantially increase the amount of SW which can be absorbed. Freeze up being later does not have this amplifying effect, as by then the available SW is approaching the near-zero winter minimum.

Figure 1g shows annual mean oceanic heat flux, including the stratification and ACC corrections. Estimates for the last years (2014 to 2018) are all greater than $5x10^{20}$J (as is 2007), with 2017 yielding the record length maximum of almost $6x10^{20}$J. Trends in annual means are significant, increasing, and greater in recent years (1991-2018: $8.3\pm3.9x10^{18}$J/yr; 2000-2018: $11.1\pm5.3x10^{18}$J/yr). Although not all this heat may be lost to ice melt, $6x10^{20}$J of heat could melt $2x10^{6}$km^2 of 1m thick ice. (For scale note the seasonal change in Arctic sea-ice extent is ~$10x10^{6}$km^2). Prior work suggests the Bering Strait heat flux acts as a trigger of the onset of ice melt [*Woodgate et al.*, 2010; *Lu et al.*, 2020], and that spring (April-June) and autumn (July-

September) ocean heat fluxes are the best available predictors of Chukchi summer melt-back and winter ice advance respectively [*Serreze et al.*, 2016]. Monthly heat flux trends (Figure 2e, column 1) are largest in both these critical periods.

Finally, note that the total oceanic heat flux delivered to the Arctic by Pacific waters (see also *Danielson et al.*, [2020b]) must be the sum of the oceanic heat through the strait and the net surface fluxes (i.e., to the water) in the Chukchi Sea, the dominant warming of which is the incoming shortwave (SW) [*Serreze et al.*, 2007]. While results [*Woodgate et al.*, 2010] suggest the magnitude of interannual variability of both incoming SW and Bering Strait heat is currently comparable, remember that the SW input has an upper limit, viz., the incoming SW for an entirely ice-free situation and can, at most, likely only double from its current contribution. In contrast, the oceanic heat flux has much more capacity to increase, as it is limited merely by the temperature of the incoming waters from the south, which has already risen (in the annual mean) from only 1°C above freezing to about 3°C above freezing between 1991 and 2018 (Figure 1c).

5 Freshening, increasing freshwater fluxes and loss of winter ventilation of the Arctic's lower halocline

Figure 1h shows significant freshening trends in annual mean near-bottom salinities at A3 (black, -0.015±0.008psu/yr) and A2 (grey, -0.011±0.009psu/yr). These trends yield large salinity changes over the time-series (e.g., at A3, from >32.7psu in the 1990s to <32.3psu since 2015). Monthly data (Figure 2c, first column) show this change is almost entirely in the winter/spring months (Jan-Mar, ~0.03psu/yr), with summer salinities showing no significant freshening. This winter freshening is sufficiently dramatic to alter the extrema of the annual cycle (Figure 2c, columns 2-4). The 1990-2004 climatology (*Woodgate et al.*, [2005b], black) showed maximum salinities in March, with winter (January to March) salinization, attributed to brine rejection on ice formation. However, recent years (red) show winter salinities >1psu fresher than climatology, completely eroding the climatological winter maximum and yielding instead maximum salinities in the summer.

Combined with hourly transport estimates and stratification and ACC corrections (Figure 1i), this freshening yields significantly increasing freshwater fluxes (35±17km^3/yr), with recent annual mean fluxes around 3000-3500km^3. Thus, in times of Arctic freshening [*Haine et al.*, 2015], the Bering Strait maintains its role as a key (order 1/3rd) contributor of freshwater input to the Arctic, with interannual variability around 1000km^3, greater than variability in any other source [*Woodgate et al.*, 2015].

What causes this freshening? It seems unlikely to be due to sea-ice change, since it appears as a freshening in winter, which in magnitude would require net import of ~700km^3 more ice into the region now than in the 1990s, a volume comparable to the total ice volume of the Bering Sea (~800km^3, [*Zhang et al.*, 2010]). (While ice advection within the Bering Sea is larger (~1500km^3/yr, [*Pease*, 1980; *Zhang et al.*, 2010]), the vast majority of this ice is melted within the Bering Sea, whereas for the Bering Strait changes observed, new ice would need to be advected into the system.) It cannot be due to less ice formation, as the signal is a freshening from summer values, not just a reduction in winter salinization. In any case, since the change is also present in the annual mean, it cannot be due to seasonal sea ice change, but requires advection of fresher waters into the system.

A 0.5psu change to 1Sv of 32.7psu water requires ~500km^3 extra freshwater. The Yukon (the major river input to the region), is only ~220km^3/yr, with interannual variability of around 20km^3 and no significant trend over the period considered (Pilot Station data from waterdata.usgs.gov). A volume and salt budget analysis [*Aagaard et al.*, 2006] suggests only two other significant sources - on-shelf flow from the Bering Sea (saltier than the Bering Strait) and the Unimak Pass inflow (fresher than the strait) in the southern Bering Sea. Since we observe both flow increase and freshening, this makes increasing/freshening Unimak Pass inflow the most likely driver of the Bering Strait freshening, and indeed significant freshening (~3psu from 1990 to end of study, 2005) of the Unimak Pass waters is indicated by coralline algal chemistry [*Chan et al.*, 2011], attributed to increased glacial melt and precipitation from mainland Alaska. Note that the timing (winter) of freshening in the strait is consistent with the likely several month transit time of a summer fresh signal in Unimak Pass across the ~1300km to the strait.

The possible impacts on the Arctic of this Bering Strait freshening are dramatic. The 30-day smoothed density from near-bottom A3 (Figure 3a) clearly shows change from the high density (σ>26.5kg/m^3, green) winter waters of the 1990s to much less dense waters in the more recent years (maximum σ<26.2kg/m^3, magenta). This corresponds to a ~50m shoaling of equilibrium depth in the Arctic from ~100-150m to ~50-100m [*Pickart et al.*, 2011, Figure 7]. Unless this freshening can be compensated by processes in the Chukchi, this implies loss of the denser fractions ventilating the Arctic water column.

Sufficient compensating salinization in the Chukchi seems unlikely. It would require ~700km^3 more Chukchi ice formation and export than in the 1990s. Assuming 1m thick ice, that corresponds to about twice the area of the Chukchi Sea [*Jakobsson*, 2002]) - an unrealistic amount of increase. Additionally, satellite and mooring data [*Travers*, 2012, updated] suggest instead thinning and reduced ice extent in the region [*Perovich et al.*, 2019]. Thus it seems inescapable that this freshening in the strait must translate to freshening in the Pacific ventilation of the Arctic water column.

A typical annual volumetric temperature-salinity (TS) plot (A3 data) of the early 1990s (Figure 3b, column 1) shows two major water classes, a warmer (~1°C), fresher (~32.7psu) summer water (σ~26.2kg/m^3), clearly distinct from a denser (σ>26.5kg/m^3), saltier (>33psu) contribution at the freezing temperature. Notably the colder waters are saltier (blue, Figure 3b, middle 1991 plot) and thus denser (blue, Figure 3b, right 1991 plot) than their warmer (red lines) summer counter parts. But in recent years (Figure 3b, 2018 example, column 1), the TS juxtaposition of summer and winter water is vastly altered. The winter waters at freezing are now on comparable isopycnals to the summer water (Figure 3b, 2018 left and right plots) and cold (blue) waters occupy a fresher salinity bracket than the summer waters (Figure 3b, middle 2018 plot).

To quantify this change interannually (Figure 3c), we split the total annual transport (grey) into portions less/more dense than the traditional summer water of 26.2kg/m^3 (magenta pluses/ dashed black respectively), showing also the amount of water at or more dense than the old winter ventilation density of 26.5kg/m^3 (green circles). This calculation suggests dense water ventilation has dwindled from 0.2-0.4Sv per year in the 1990s to almost zero since 2014.

This implies some dramatic changes to how Pacific waters ventilate the Arctic water column (Figure 3e):

1) Pacific Winter Water (PWW) no longer renews the traditional cold halocline layer at 33.1psu (Figure 3d), but instead mixes with the Pacific Summer Water at lesser densities and shallower depths.

2) PWW, traditionally high in nutrients, is likely entering the Arctic water column at depths of ~50-100m instead of 100-150m, making its nutrient (and other chemical) loads more accessible to the surface layers of the Arctic.

6 Summary and Conclusions

Near-bottom, year-round mooring data show continuing increasing trends in the Pacific inflow to the Arctic from 1990 to the end of current data (summer 2019), with flow increase being primarily due to the far-field (pressure-head) forcing of the flow. There is a clear warming, especially in recent years, yielding a net heat inflow of around $6x10^{20}$J/year in 2017 and 2018 (Figure 1i). This is near surface heat, available to melt ice. Observed trends to earlier ice melt may allow a greater contribution of SW to the oceanic heating of the Chukchi (trends to later freeze-up have less impact on absorbed SW), although the total SW contribution is bounded by ice-free conditions, whereas oceanic heat flux is less constrained.

More unexpected, however, is the dramatic freshening of the throughflow, and its implications for the Arctic - viz., ventilation depths shoaling from ~100-150m to 50-100m, and particularly lack of ventilation of the Arctic's cold halocline at 33.1psu. This implies a restructuring of the upper Arctic Ocean water column. While it is possible the cold halocline may merely reform fresher, it is notable that summer Pacific waters are now of the same density as winter waters, hindering the formation of a uniformly cold layer as currently isolates the Arctic ice from the warmth of the Atlantic water below. In any case, given little change in the salinity and density of incoming Atlantic water, freshening of the Pacific inflow suggests enhanced stratification in the Arctic surface layers, likely inhibiting wind-driven mixing [*Peralta-Ferriz and Woodgate*, 2015].

These results are supported by scarcer upper layer observations of the ACC and stratification.

We note finally that few models manage to recreate these observed trends in the Bering Strait flow, especially increasing flow in recent years. *Jahn and Laiho* [2020], for example, using climate models suggest trends in the Bering Strait should not be significant until ~2050, although they are significant now in our observations. Even high resolution Arctic models match only variability and not trend [*Nguyen et al.*, 2020]. This suggests models are still unable to capture both the drivings and the implications of change in the Pacific inflow to the Arctic, and emphasizes both the need to improve model simulations of the throughflow and to continue the *in situ* observational record.

Acknowledgments and Data

This work was supported by NSF Arctic Observing Network grants PLR-1304052 and PLR-1758565. The Bering Strait mooring data are permanently archived at the National Centers for Environmental Information (ncei.noaa.gov), with data and products available at the Bering Strait project website, psc.apl.washington.edu/BeringStrait.html.

Figure 1:

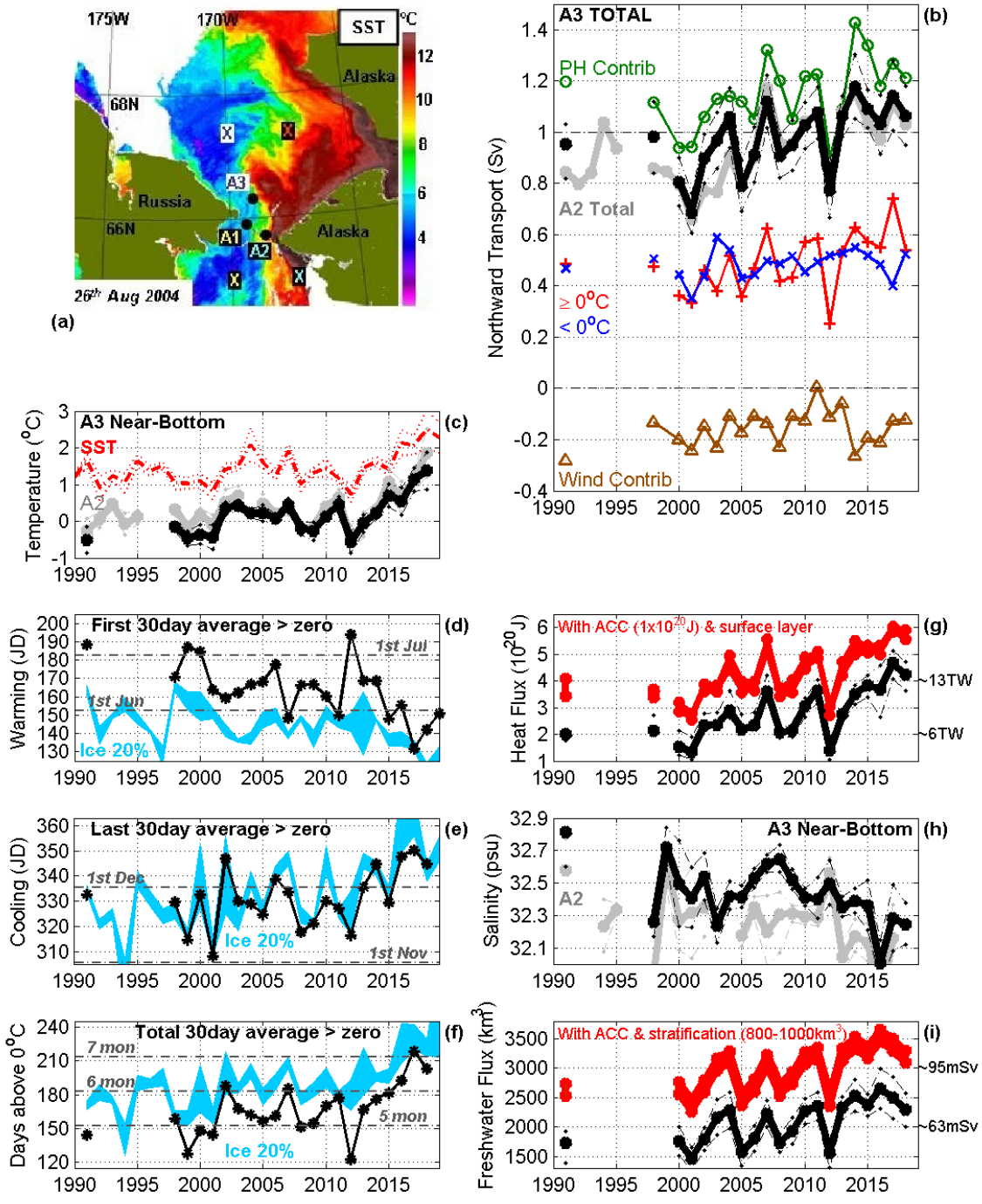

Figure 1. Annual mean Bering Strait properties. **(a)** Summer satellite (MODIS) Sea Surface Temperature (SST) image of the Bering Strait region showing moorings (black dots) and NCEP wind points (X) [from *Woodgate et al.*, 2010]. **(b)** Total northward volume transport estimated from A2 (grey) and from A3 with corrections (black, with uncertainty dashed), the latter split into volume colder than (blue crosses) or at/warmer than (red pluses) 0°C, and into the pressure-

head (green circles) or local wind-driven (brown triangles) contributions. From A3 (black) and A2 data (grey), annual mean **(c)** near-bottom temperature with SST (red); **(h)** salinity; **(g,i)** heat and freshwater transports respectively, with corrections (red) for the Alaskan Coastal Current (ACC) and surface layer/stratification. From 30-day smoothed A3 data, first **(d)** and last **(e)** Julian day (JD) above 0°C and number of days above 0°C **(f)**, showing (blue) when 30-day smoothed SSM/I ice concentration at A3 first/last falls below 20% (melt-back) **(d)**; rises above 20% (freeze-up) **(e)**, and open water time between these dates **(f)**.

Figure 2:

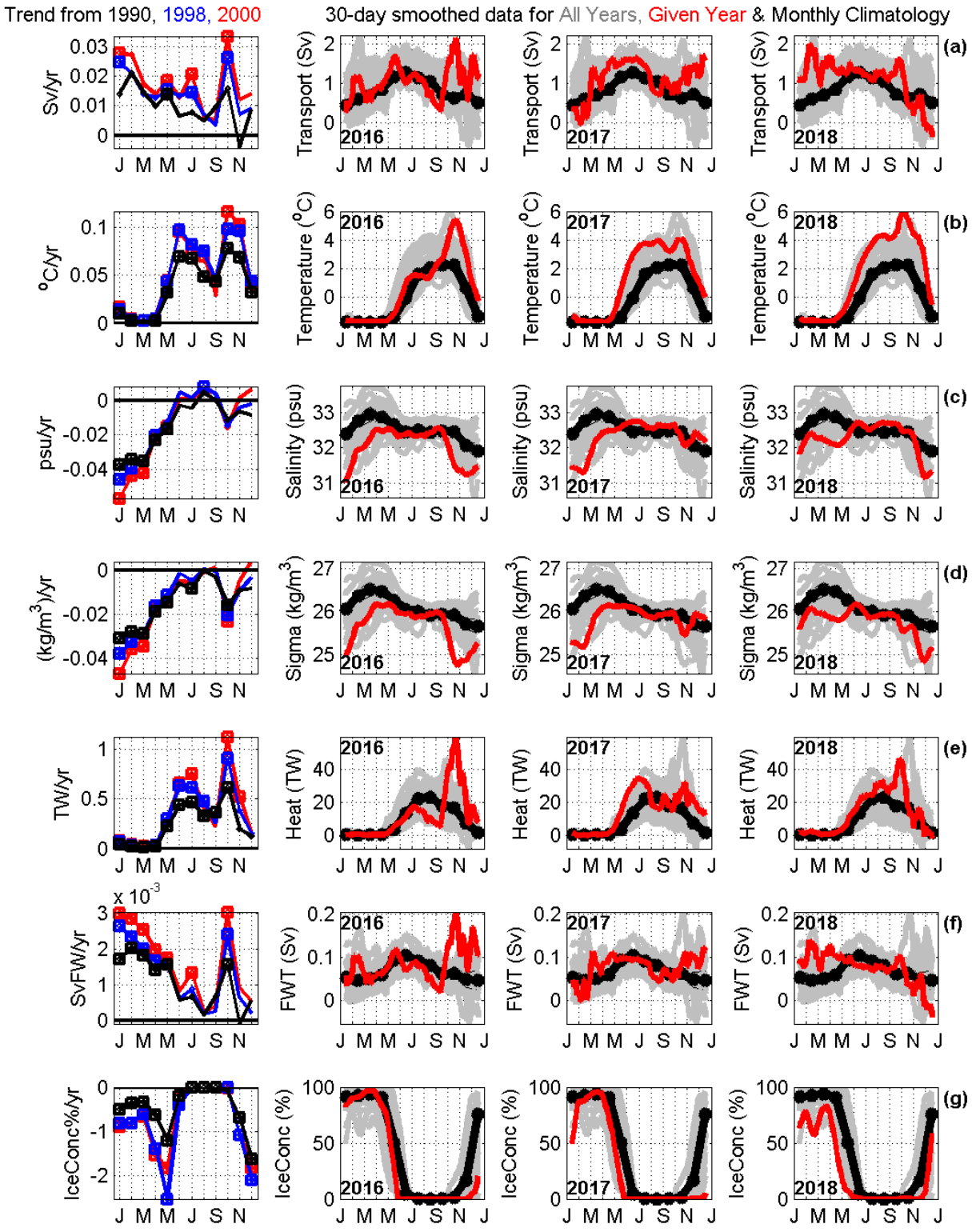
Trend from 1990, 1998, 2000
30-day smoothed data for All Years, Given Year & Monthly Climatology
Sv/yr
Transport (Sv)
(a)
°C/yr
Temperature (°C)
(b)
psu/yr
Salinity (psu)
(c)
(kg/m3)/yr
Sigma (kg/m3)
(d)
TW/yr
Heat (TW)
(e)
x 10-3
SvFW/yr
FWT (Sv)
(f)
IceConc%/yr
IceConc (%)
(g)
2016
2017
2018
J M M J S N J

Figure 2. Trends and recent change in Bering Strait properties of A3 **(a)** transport, **(b)** temperature, **(c)** salinity, **(d)** density, **(e)** heat transport, **(f)** freshwater transport (FWT) and **(g)** % SSM/I ice concentration at A3. **First column**: trend per month (large squares if significant) from 1990 (black), 1998 (blue), and 2000 (red) to end of present data (summer 2019). **Last three columns**: 30-day A3 data for 2016, 2017 and 2018 (red); all prior data (grey), and the 1990-2004 climatology of ice or water properties [*Woodgate et al.*, 2005b] (black).

Figure 3:

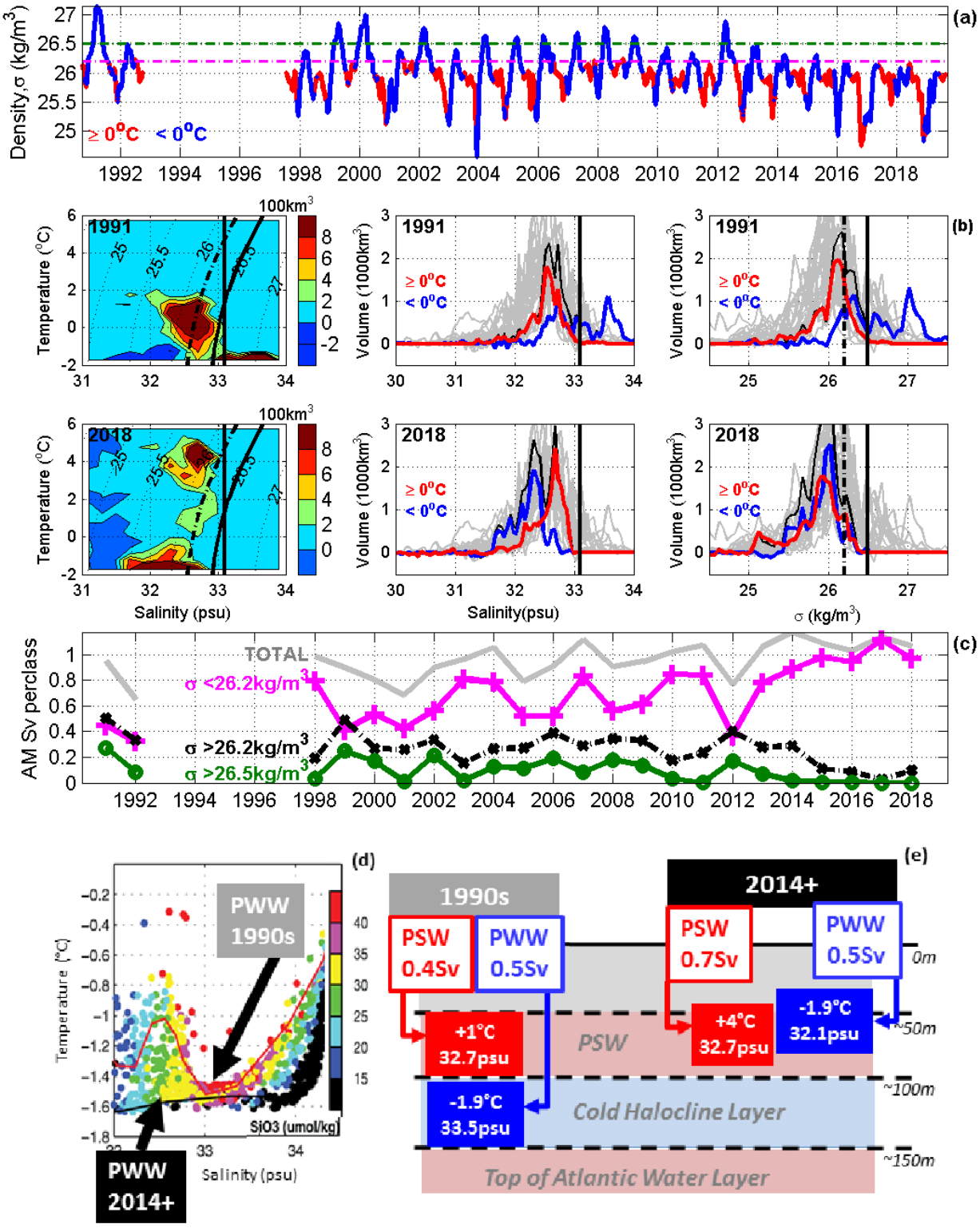
(a)
Density,σ (kg/m3)
≥ 0°C
< 0°C
(b)
1991
2018
Temperature (°C)
Volume (1000km3)
100km3
Salinity (psu)
σ (kg/m3)
(c)
AM Sv perclass
TOTAL
σ <26.2kg/m3
σ >26.2kg/m3
σ >26.5kg/m3
(d)
PWW 1990s
PWW 2014+
Temperature (°C)
Salinity (psu)
SiO3 (umol/kg)
(e)
1990s
2014+
PSW 0.4Sv
PWW 0.5Sv
PSW 0.7Sv
PWW 0.5Sv
+1°C 32.7psu
+4°C 32.7psu
-1.9°C 32.1psu
-1.9°C 33.5psu
PSW
Cold Halocline Layer
Top of Atlantic Water Layer
0m
~50m
~100m
~150m

Figure 3. **(a)** Thirty-day smoothed A3 near-bottom density for waters at/warmer than (red) or colder than (blue) 0°C. **(b)** For 1991 (top) and 2018 (bottom) volumetric temperature-salinity (TS) plot (left) and volume in salinity (middle) and density (right) classes, summed for waters at/warmer than (red) or colder than (blue) 0°C. **(a) and (b)** mark salinity and density thresholds discussed in Section 5. **(c)** Annual mean transports (from A3) in density classes: total (grey), < 26.2kg/m^3 (magenta pluses), > 26.2 kg/m^3 (black dashed) and >26.5 kg/m^3 (green circles). **(d)** TS plot for 2002 waters north of the Chukchi slope colored by silicate (indicating Pacific influence) [modified from *Woodgate et al.*, 2005c], marking changing TS of Pacific Winter Waters (PWW). **(e)** Schematic of changing ventilation from PWW and Pacific Summer Water (PSW).

References

Aagaard, K., and E. C. Carmack (1989), The role of sea ice and other fresh water in the Arctic circulation, *J. Geophys. Res.*, *94*(C10), 14485-14498.

Aagaard, K., L. K. Coachman, and E. Carmack (1981), On the halocline of the Arctic Ocean, *Deep-Sea Res., Part A*, *28*(6A), 529-545.

Aagaard, K., T. J. Weingarter, S. Danielson, R. A. Woodgate, G. C. Johnson, and T. Whitledge (2006), Some controls on flow and salinity in Bering Strait, *Geophys. Res. Lett.*, *33*, L19602, doi: 10.1029/2006GL026612.

Cavalieri, D. J., C. L. Parkinson, P. Gloersen, and H.Zwally (1996), Sea Ice Concentrations from Numbus-7 SMMR and DMSP SSM/I-SSMIS Passive Microwave Data (1979-2012), edited, NASA DAAC at the National Snow and Ice Data Center, Boulder, Colorado, USA.

Chan, P., J. Halfar, B. Williams, S. Hetzinger, R. Steneck, T. Zack, and D. E. Jacob (2011), Freshening of the Alaska Coastal Current recorded by coralline algal Ba/Ca ratios, *Journal of Geophysical Research: Biogeosciences*, *116*(G1), doi: 10.1029/2010JG001548.

Coachman, L. K., and K. Aagaard (1966), On the water exchange through Bering Strait, *Limnology and Oceanography*, *11*(1), 44-59.

Danielson, S. L., T. J. Weingartner, K. S. Hedstrom, K. Aagaard, R. Woodgate, E. Curchitser, and P. J. Stabeno (2014), Coupled wind-forced controls of the Bering–Chukchi shelf circulation and the Bering Strait throughflow: Ekman transport, continental shelf waves, and variations of the Pacific–Arctic sea surface height gradient, *Prog. Oceanogr.*, *125*(0), 40-61, doi: 10.1016/j.pocean.2014.04.006.

Danielson, S. L., T. D. Hennon, K. S. Hedstrom, A. V. Pnyushkov, I. V. Polyakov, E. Carmack, K. Filchuk, M. Janout, M. Makhotin, W. J. Williams, and L. Padman (2020a), Oceanic Routing of Wind-Sourced Energy Along the Arctic Continental Shelves, *Frontiers in Marine Science*, *7*(509), doi: 10.3389/fmars.2020.00509.

Danielson, S. L., O. Ahkinga, C. Ashjian, E. Basyuk, L. W. Cooper, L. Eisner, E. Farley, K. B. Iken, J. M. Grebmeier, L. Juranek, G. Khen, S. R. Jayne, T. Kikuchi, C. Ladd, K. Lu, R. M. McCabe, G. W. K. Moore, S. Nishino, F. Ozenna, R. S. Pickart, I. Polyakov, P. J. Stabeno, R. Thoman, W. J. Williams, K. Wood, and T. J. Weingartner (2020b), Manifestation and consequences of warming and altered heat fluxes over the Bering and Chukchi Sea continental shelves, *Deep Sea Research Part II: Topical Studies in Oceanography*, *177*, 104781, doi: 10.1016/j.dsr2.2020.104781.

Haine, T. W. N., B. Curry, R. Gerdes, E. Hansen, M. Karcher, C. Lee, B. Rudels, G. Spreen, L. de Steur, K. D. Stewart, and R. Woodgate (2015), Arctic freshwater export: Status, mechanisms, and prospects, *Global and Planetary Change*, *125*(0), 13-35, doi: 10.1016/j.gloplacha.2014.11.013.

Jahn, A., and R. Laiho (2020), Forced Changes in the Arctic Freshwater Budget Emerge in the Early 21st Century, *Geophys. Res. Lett.*, *47*(15), e2020GL088854, doi: 10.1029/2020GL088854.

Jakobsson, M. (2002), Hypsometry and volume of the Arctic Ocean and its constituent seas, *Geochem. Geophys. Geosyst.*, *3*, doi: 10.1029/2001GC000302.

Kalnay, E., M. Kanamitsu, R. Kistler, W. Collins, D. Deaven, L. Gandin, M. Iredell, S. Saha, G. White, J. Woollen, Y. Zhu, M. Chelliah, W. Ebisuzaki, W. Higgins, J. Janowiak, K. C. Mo, C. Ropelewski, J. Wang, A. Leetmaa, R. Reynolds, R. Jenne, and D. Joseph (1996), The NCEP/NCAR 40-Year Reanalysis Project, *Bulletin of the American Meteorological Society*, *77*(3), 437-472, doi: 10.1175/1520-0477(1996)077<0437:tnyrp>2.0.co;2.

Levine, R. M., A. De Robertis, D. Grünbaum, R. Woodgate, C. W. Mordy, F. Mueter, E. Cokelet, N. Lawrence-Slavas, and H. Tabisola (2020), Autonomous vehicle surveys indicate that flow reversals retain juvenile fishes in a highly advective high-latitude ecosystem, *Limnology and Oceanography*, *n/a*(n/a), doi: https://doi.org/10.1002/lno.11671.

Lu, K., S. Danielson, K. Hedstrom, and T. Weingartner (2020), Assessing the role of oceanic heat fluxes on ice ablation of the central Chukchi Sea Shelf, *Prog. Oceanogr.*, *184*, 102313, doi: 10.1016/j.pocean.2020.102313.

Nguyen, A. T., R. A. Woodgate, and P. Heimbach (2020), Elucidating Large-Scale Atmospheric Controls on Bering Strait Throughflow Variability Using a Data-Constrained Ocean Model and Its Adjoint, *J. Geophys. Res. -Ocean*, *125*(9), e2020JC016213, doi: https://doi.org/10.1029/2020JC016213.

Østerhus, S., R. Woodgate, H. Valdimarsson, B. Turrell, L. de Steur, D. Quadfasel, S. M. Olsen, M. Moritz, C. M. Lee, K. M. H. Larsen, S. Jónsson, C. Johnson, K. Jochumsen, B. Hansen, B. Curry, S. Cunningham, and B. Berx (2019), Arctic Mediterranean exchanges: a consistent volume budget and trends in transports from two decades of observations, *Ocean Sci.*, *15*(2), 379-399, doi: 10.5194/os-15-379-2019.

Paquette, R. G., and R. H. Bourke (1974), Observations on the Coastal Current of Arctic Alaska, *J. Mar. Res.*, *32*(2), 195-207.

Pease, C. H. (1980), Eastern Bering Sea Ice Processes, *Monthly Weather Review*, *108*, 2015-2023.

Peralta-Ferriz, C., and R. A. Woodgate (2015), Seasonal and interannual variability of pan-Arctic surface mixed layer properties from 1979 to 2012 from hydrographic data, and the dominance of stratification for multiyear mixed layer depth shoaling, *Prog. Oceanogr.*, *134*, 19-53, doi: 10.1016/j.pocean.2014.12.005.

Peralta-Ferriz, C., and R. A. Woodgate (2017), The Dominant Role of the East Siberian Sea in Driving the Oceanic Flow Through the Bering Strait—Conclusions From GRACE Ocean Mass Satellite Data and In Situ Mooring Observations Between 2002 and 2016, *Geophys. Res. Lett.*, doi: 10.1002/2017gl075179.

Perovich, D., W. Meier, M. Tschudi, S. Farrell, S. Hendricks, S. Gerland, L. Kaleschke, R. Ricker, X. Tian-Kunze, M. Webster, and K. Wood (2019), Sea Ice, in *Arctic Report Card 2019*, edited by J. Richter-Menge, M.L.Druckenmiller and M.Jeffries, http://www.arctic.noaa.gov/Report-Card.

Pickart, R. S., M. A. Spall, G. W. K. Moore, T. J. Weingartner, R. A. Woodgate, K. Aagaard, and K. Shimada (2011), Upwelling in the Alaskan Beaufort Sea: Atmospheric forcing and local versus non-local response, *Prog. Oceanogr.*, *88*(1-4), 78-100, doi: doi:10.1016/j.pocean.2010.11.005.

Reynolds, R. W., T. M. Smith, C. Liu, D. B. Chelton, K. S. Casey, and M. G. Schlax (2007), Daily high-resolution-blended analyses for sea surface temperature, *J. Climate*, *20*(22), 5473-5496, doi: 10.1175/2007jcli1824.1.

Serreze, M. C., A. D. Crawford, J. Stroeve, A. P. Barrett, and R. A. Woodgate (2016), Variability, trends, and predictability of seasonal sea ice retreat and advance in the Chukchi Sea, *J. Geophys. Res. -Ocean*, 18pp, doi: 10.1002/2016jc011977.

Serreze, M. C., A. P. Barrett, A. G. Slater, M. Steele, J. Zhang, and K. E. Trenberth (2007), The large-scale energy budget of the Arctic, *J. Geophys. Res.*, *112*(C11122), doi:10.1029/2006JD008230.

Steele, M., J. Morison, W. Ermold, I. Rigor, M. Ortmeyer, and K. Shimada (2004), Circulation of summer Pacific halocline water in the Arctic Ocean, *J. Geophys. Res.*, *109*(C2), C02027, doi: 10.1029/2003JC002009.

Thoman, R. L., J. Richter-Menge, and M. L. Druckmiller (2020), Arctic Report Card 2020, 143, doi: 10.25923/mn5p-t549.

Travers, C. S. (2012), Quantifying Sea-Ice Volume Flux using Moored Instrumentation in the Bering Strait, 85 pp, University of Washington, available at http://psc.apl.washington.edu/HLD.

Walsh, J. J., D. A. Dieterle, F. E. Muller-Karger, K. Aagaard, A. T. Roach, T. E. Whitledge, and D. Stockwell (1997), CO2 cycling in the coastal ocean. II. Seasonal organic loading of the Arctic Ocean from source waters in the Bering Sea, *Continental Shelf Research, 17*(1), 1-36.

Woodgate, R. A. (2018), Increases in the Pacific inflow to the Arctic from 1990 to 2015, and insights into seasonal trends and driving mechanisms from year-round Bering Strait mooring data, *Prog. Oceanogr., 160*, 124-154, doi: 10.1016/.pocean.2017.12.007.

Woodgate, R. A., and K. Aagaard (2005), Revising the Bering Strait freshwater flux into the Arctic Ocean, *Geophys. Res. Lett., 32*(2), L02602, doi: 10.1029/2004GL021747.

Woodgate, R. A., K. Aagaard, and T. J. Weingartner (2005a), A year in the physical oceanography of the Chukchi Sea: Moored measurements from autumn 1990-1991, *Deep-Sea Res., Part II, 52*(24-26), 3116-3149, doi: 10.1016/j.dsr2.2005.10.016.

Woodgate, R. A., K. Aagaard, and T. J. Weingartner (2005b), Monthly temperature, salinity, and transport variability of the Bering Strait throughflow, *Geophys. Res. Lett., 32*(4), L04601, doi: 10.1029/2004GL021880.

Woodgate, R. A., T. J. Weingartner, and R. W. Lindsay (2010), The 2007 Bering Strait Oceanic Heat Flux and anomalous Arctic Sea-ice Retreat, *Geophys. Res. Lett., 37*, L01602, doi: 10.1029/2009GL041621.

Woodgate, R. A., K. M. Stafford, and F. G. Prahl (2015), A Synthesis of Year-Round Interdisciplinary Mooring Measurements in the Bering Strait (1990–2014) and the RUSALCA Years (2004–2011), *Oceanography*, *28*(3), 46-67, doi: 10.5670/oceanog.2015.57.

Woodgate, R. A., K. Aagaard, J. H. Swift, K. K. Falkner, and W. M. Smethie (2005c), Pacific ventilation of the Arctic Ocean's lower halocline by upwelling and diapycnal mixing over the continental margin, *Geophys. Res. Lett., 32*(18), L18609, doi: 10.1029/2005GL023999.

Zhang, J., R. Woodgate, and R. Moritz (2010), Sea Ice Response to Atmospheric and Oceanic Forcing in the Bering Sea, *J. Phys. Oceanogr., 40*(8), 1729-1747, doi: 10.1175/2010JPO4323.1